Report

Cell Reports

A Lupus-Associated Mac-1 Variant Has Defects in Integrin Allostery and Interaction with Ligands under Force

Graphical Abstract

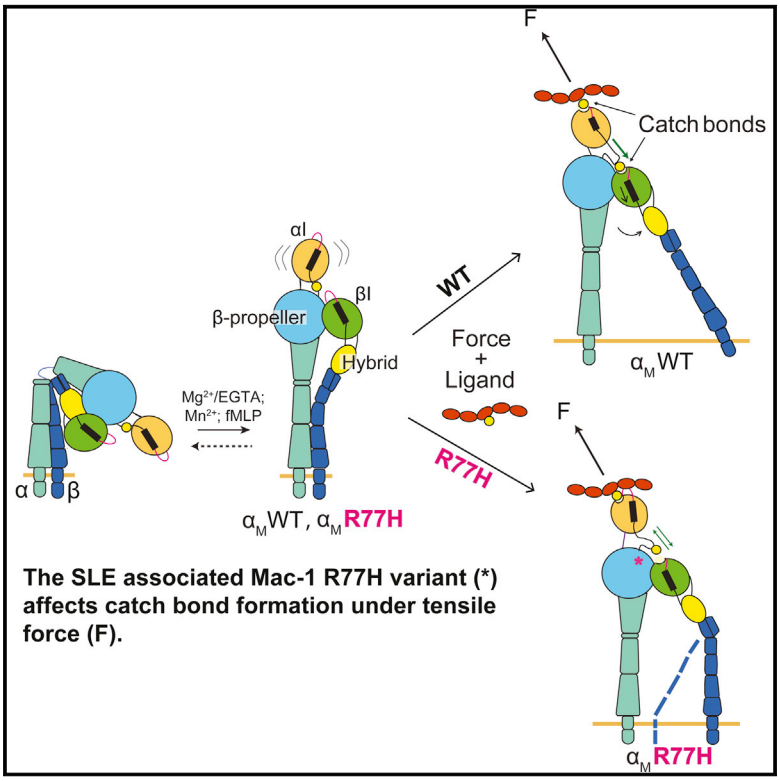

The SLE associated Mac-1 R77H variant (*) affects catch bond formation under tensile force (F).

Highlights

- The lupus risk SNP, R77H, impairs Mac-1 affinity for ligand
- R77H inhibits force-induced allosteric relay, prolonging Mac-1/ligand bond lifetime
- The β-propeller domain contributes to the relay of allostery in Mac-1
- Defects in R77H are rescued by integrin-activating antibody and tail mutations

Authors

Florencia Rosetti, Yunfeng Chen, ..., Cheng Zhu, Tanya N. Mayadas

Correspondence

cheng.zhu@bme.gatech.edu (C.Z.), tmayadas@rics.bwh.harvard.edu (T.N.M.)

In Brief

Rosetti et al. show that the Mac-1 lupus risk variant rs1143679 (R77H), located outside the Mac-1 ligand binding αI-domain, is primarily defective in binding to ligand under flow. This correlates with impaired 2D ligand affinity and catch-bond formation.

Rosetti et al., 2015, Cell Reports *10*, 1655–1664
March 17, 2015
http://dx.doi.org/10.1016/j.celrep.2015.02.037

CellPress

Cell Reports
Report

A Lupus-Associated Mac-1 Variant Has Defects in Integrin Allostery and Interaction with Ligands under Force

Florencia Rosetti,[1,2,7] Yunfeng Chen,[3,4,7] Mehmet Sen,[5] Elizabeth Thayer,[1] Veronica Azcutia,[1] Jan M. Herter,[1] F. William Luscinskas,[1] Xavier Cullere,[1] Cheng Zhu,[3,4,6,*] and Tanya N. Mayadas[1,*]

[1]Department of Pathology, Center for Excellence in Vascular Biology, Brigham and Women's Hospital and Harvard Medical School, Boston, MA 02115, USA

[2]Immunology Graduate Program, Division of Medical Sciences, Harvard Graduate School of Arts and Sciences, Harvard Medical School, Boston, MA 02115, USA

[3]Woodruff School of Mechanical Engineering, Georgia Institute of Technology, Atlanta, GA 30332, USA

[4]Institute for Bioengineering and Bioscience, Georgia Institute of Technology, Atlanta, GA 30332, USA

[5]Program in Cellular and Molecular Medicine, Department of Pediatrics, Children's Hospital, Harvard Medical School, Boston, MA 02115, USA

[6]Coulter Department of Biomedical Engineering, Georgia Institute of Technology, Atlanta, GA 30332, USA

[7]Co-first author

*Correspondence: cheng.zhu@bme.gatech.edu (C.Z.), tmayadas@rics.bwh.harvard.edu (T.N.M.)

http://dx.doi.org/10.1016/j.celrep.2015.02.037

SUMMARY

Leukocyte CD18 integrins increase their affinity for ligand by transmitting allosteric signals to and from their ligand-binding αI domain. Mechanical forces induce allosteric changes that paradoxically slow dissociation by increasing the integrin/ligand bond lifetimes, referred to as catch bonds. Mac-1 formed catch bonds with its ligands. However, a Mac-1 gene (*ITGAM*) coding variant (rs1143679, R77H), which is located in the β-propeller domain and is significantly associated with systemic lupus erythematosus risk, exhibits a marked impairment in 2D ligand affinity and affinity maturation under mechanical force. Targeted mutations and activating antibodies reveal that the failure in Mac-1 R77H allostery is rescued by induction of cytoplasmic tail separation and full integrin extension. These findings demonstrate roles for R77, and the β-propeller in which it resides, in force-induced allostery relay and integrin bond stabilization. Defects in these processes may have pathological consequences, as the Mac-1 R77H variant is associated with increased susceptibility to lupus.

INTRODUCTION

Leukocyte integrins, which are composed of a unique α complexed to a common β_2 subunit, are a major family of adhesive receptors. The regulation of their affinity for ligands is of key importance for cell adhesion and occurs through structural changes in their extracellular domains. These allosteric changes are induced upon cell activation by chemokines, ligand binding, and cytoplasmic regulators (Carman and Springer, 2003), and can also be induced by mechanical forces that prolong the lifetime of receptor-ligand bonds (Chen et al., 2010; Choi et al., 2014; Fiore et al., 2014; Kong et al., 2009), a counterintuitive phenomenon called catch bonds (Sokurenko et al., 2008). Catch bonds may allow leukocytes to roll stably and adhere firmly to the vessel wall, and to migrate and form an immunological synapse with antigen-presenting cells (Choi et al., 2014; Sokurenko et al., 2008; Liu et al., 2014). Humans who lack β_2 integrins (leukocyte adhesion deficiency I [LADI]) or intracellular molecules required for integrin activation (LADIII) exhibit significant defects in host defense, demonstrating the importance of integrins and their activation in immune cell function (Abram and Lowell, 2009). However, to date, there is no evidence that alterations in integrin allostery or catch bonds have pathological consequences in humans.

In two independent mouse models of systemic lupus erythematosus (SLE), a multi-organ autoimmune disease (Tsokos, 2011), Mac-1 ($\alpha_M\beta_2$) deficiency was shown to increase susceptibility to developing nephritis (Kevil et al., 2004; Rosetti et al., 2012). In humans, genome-wide association studies identified variants of the *ITGAM* gene, which encodes the integrin alpha-M (α_M) chain, as risk factors for SLE (Hom et al., 2008). Despite the identification of several Mac-1 SNPs, a strong risk effect was mapped to rs1143679, which results in the substitution of arginine for a histidine at position 77 (R77H) (Han et al., 2009). Although the R77H variant compromises the adhesive functions of Mac-1 to various extents (Fagerholm et al., 2013; Zhou et al., 2013), the molecular mechanism underlying the effect of this variant (which is located in the β-propeller outside of the ligand-binding αI domain) on ligand binding is unclear. Ligand binding by Mac-1 is contained within the αI domain, inserted in the β-propeller domain of the α subunit. The homologous αI and the β_2-subunit βI domains bind Mg^{2+} at their metal ion-dependent adhesion sites (MIDAS), which coordinates an invariant Glu or Asp shared by integrin ligands. Integrin activation

leads to cytoplasmic α/β tail separation and integrin extension. The extension facilitates the sequential outward movement of the hybrid domain, the downward shift of the βI α7 helix, and the opening of the βI domain, which enhances βI-MIDAS binding to the C terminus of the αI domain α7 helix invariant Glu, which serves as an internal ligand. Internal ligand binding leads to a downward shift of the αI α7 helix and thus activation of the αI MIDAS for high-affinity binding of the external ligand (Carman and Springer, 2003).

Here, we demonstrate that the Mac-1 R77H variant reduces 2D ligand-binding affinity and force-regulated dissociation of receptor-ligand bonds (catch bonds). The latter is rescued by mutations and an activating antibody distal to R77H that are documented to induce integrin allosteric changes, indicating that R77H regulates integrin allostery, which is needed to prolong the lifetime of adhesive bonds under shear flow. A reduction in Mac-1's binding affinity and bond stability may impact Mac-1 function and thus contribute to lupus susceptibility.

RESULTS

Neutrophils Expressing the Mac-1 R77H Variant Have Defects in Neutrophil Adhesion under Hydrodynamic Forces

The crystal structure of the sister integrin $\alpha_X\beta_2$ (Sen et al., 2013), which is 60% identical to Mac-1 (Yu et al., 2012), was used to model Mac-1. Domains were further adjusted using the open headpiece of $\alpha_{IIb}\beta_3$ integrin (Xiao et al., 2004) to make an extended-open Mac-1 integrin (Figure 1A). The R77H mutation exists in the outer rim of the β-propeller, in close proximity to the αI domain. The schematic shown in Figure 1A also contains the location of binding sites of activation reporter, functional blocking, and control antibodies used in our study.

To assess the functional repercussions of R77H, we evaluated human neutrophils homozygous for the risk (R77H; rs1143679) or non-risk variant. Surface expression of Mac-1 (Figure 1B), exposure of the α_M activation reporter epitope CBRM1/5 (Figure 1C), neutrophil activation markers, and other surface molecules (e.g., $\alpha_L\beta_2$ and CD32) (Figure S1A) were similar upon stimulation with the chemokine N-formylmethionyl-leucyl-phenylalanine (fMLP). Thus, R77H has no effect on the expression and activation of Mac-1 on neutrophils, as previously reported (Zhou et al., 2013). Adhesion assays on complement iC3b-coated surfaces were done under static or shear flow conditions following fMLP treatment. Neutrophil binding was significantly reduced by Mac-1 blocking antibodies (Table S1), and neutrophils with the R77H variant had no defects in binding under static conditions (Figure 1D), spreading (Figure 1E), or phagocytosis (data not shown). However, they exhibited a significant decrease in ligand binding under shear flow (Figure 1F). They also displayed a trend toward reduced velocity during random migration induced by shear force (Figure 1G), a Mac-1 dependent function (Phillipson et al., 2006) that, like adhesion under shear flow, requires optimal integrin on- and off-rates. These results were recapitulated with neutrophils from healthy volunteers treated with functional blocking antibodies to the β-propeller domain in which R77H resides. CBRN1/6, 3/4, and 1/32 partially affected adhesion under static conditions but abrogated ligand binding under shear flow, whereas CBRM1/20 (another β-propeller antibody) and CBR LFA1/7 (a control-binding antibody) had no effect (Figures 1H and 1I; Table S1). All antibodies bound Mac-1 similarly (Figure S1B). iC3b may also have binding sites in the β-propeller (Yalamanchili et al., 2000). However, β-propeller blockade prevented binding to both ICAM-1 and iC3b under flow (Table S1), suggesting that our results were not due solely to direct inhibition of iC3b binding to the β-propeller. Finally, both β-propeller inhibition and an antibody to the αI domain hindered the migration velocity of neutrophils (Figure 1J).

Residue R77 and the β-Propeller Are Required for Mechanical Force-Induced Adhesion in K562 Cells Expressing Mac-1

We found that 90% of the neutrophil samples that were homozygous for the R77H were also homozygous for two other SLE-associated SNPs, rs1143683 and rs1143678, which are present in the Calf-1 and cytoplasmic domain of *ITGAM*, respectively, as reported by others (Zhou et al., 2013). To assess the R77H-specific contribution, we evaluated the human leukemic cell line K562 stably expressing similar levels of $\alpha_M^{WT}\beta_2$ or $\alpha_M^{R77H}\beta_2$ (Figure S2A) and K562 cells alone after they were treated with Mg^{2+}/EGTA or Mn^{2+} to directly activate integrins (Xiao et al., 2004). Mac-1 activation, examined with activation-reporter antibodies, was similar in both groups (Figure S2B). Under static conditions, Mg^{2+}/EGTA-activated α_M^{R77H} cells had a significant defect in binding to iC3b surfaces, but Mn^{2+}-treated α_M^{WT} and α_M^{R77H} cells bound equivalently (Figure 2A), the latter being consistent with the comparable binding capacity observed in fMLP-stimulated neutrophils from risk and non-risk variants (Figure 1D). The differential requirement for R77H in the presence of Mn^{2+} versus Mg^{2+}/EGTA in static assays may reflect the occupation of all three βI-domain metal sites by Mn^{2+}, which, coupled with high ligand density, maximizes the on-rate and integrin avidity and thus bypasses the need for R77. On the other hand, Mg^{2+}/EGTA blocks the occupancy and thus the negative regulatory role of Ca^{2+} at the ADMIDAS (Xiong et al., 2003), which results in less stable internal ligand binding and requires R77 for full integrin activation. Under shear flow, R77H had a defect in binding ICAM-1 in the presence of Mg^{2+}/EGTA at shear stresses of 0.19–0.42 dynes/cm^2, with the most significant difference observed at 0.38 dynes/cm^2 (Figure S2C). Further analysis at this shear stress revealed impaired binding of α_M^{R77H} cells to iC3b or ICAM-1 in the presence of either Mn^{2+} or Mg^{2+}/EGTA (Figure 2B). In addition, although β-propeller antibodies only partially affected adhesion under static conditions, they significantly abrogated ligand binding under shear flow (Figures 2C, 2D, and S1C; Table S1). The similarity of the results obtained with human neutrophils suggests that R77H in the β-propeller is primarily responsible for the observed adhesion defects in human neutrophils.

Separation of the α- and β-Subunit Cytoplasmic Tails, but Not βI-Domain Activation, Rescues the Mac-1-R77H Binding Defect under Flow

Mutations in the βI domain of $\alpha_X\beta_2$ that increase its affinity for the αI α7-helix internal ligand result in a greater population of αI domain in the open conformation, and thus stabilize $\alpha_X\beta_2$ in an extended conformation with an open headpiece (Sen et al.,

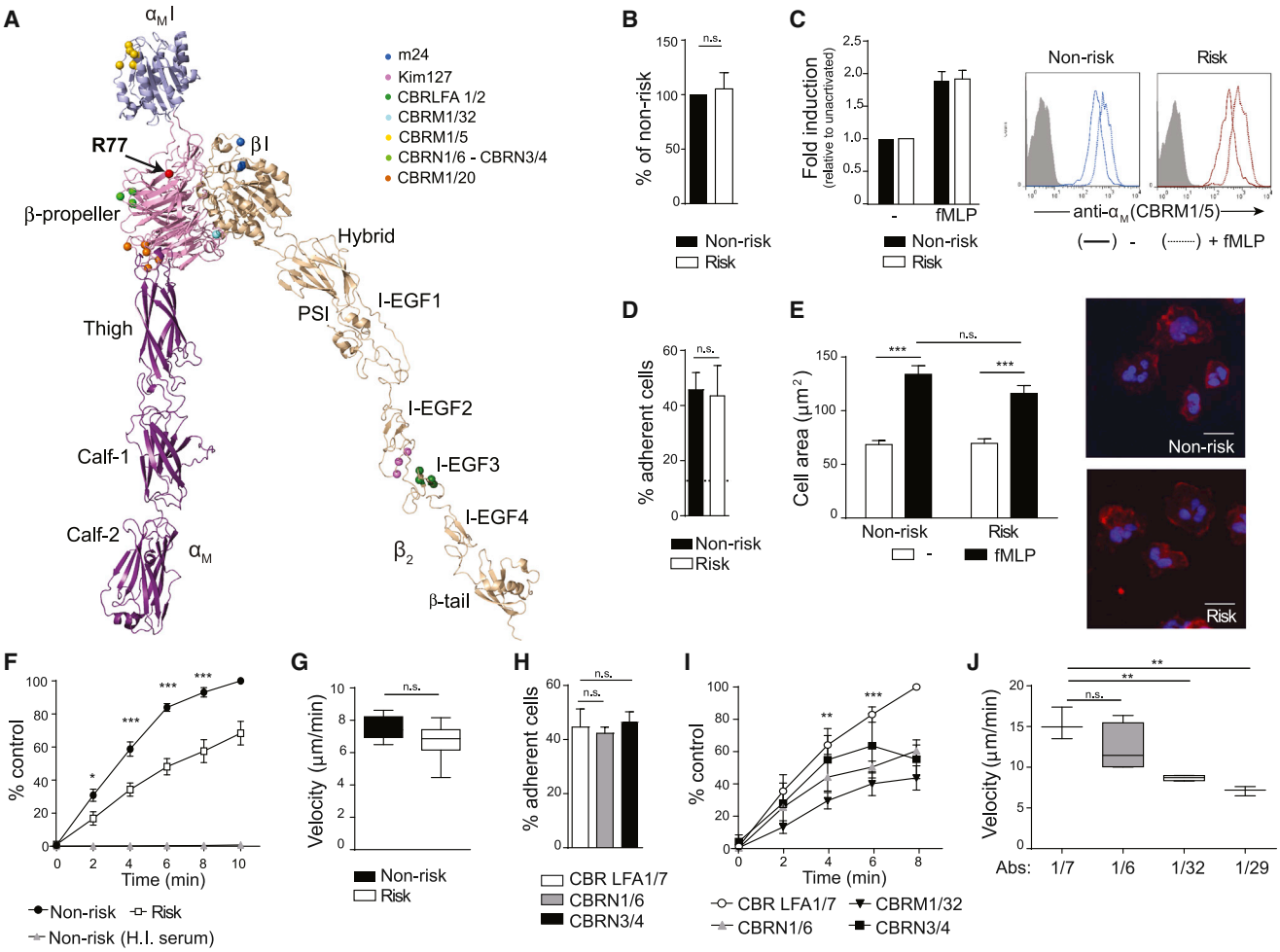

Figure 1. Functional Effects of the *ITGAM* R77H Risk Variant in Human Neutrophils

(A) Model of $\alpha_M\beta_2$ ectodomain. The R77 region (arrow) and epitopes for antibodies are indicated with color-coded spheres.

(A–G) Neutrophils from non-risk and risk-variant donors were treated with fMLP or vehicle control (–).

(B and C) Surface expression of α_M (B) and CBRM1/5 antibody binding (C) were examined by flow cytometry. Data are the fold induction relative to vehicle-treated cells. Representative histograms are shown. n = 4.

(D) Adhesion of neutrophils to an iC3b-coated surface under static conditions. The dotted line indicates binding of cells to a surface with heat-inactivated serum (H.I.). n = 4 experiments.

(E) Spreading of neutrophils on iC3b. The cell area was quantified and representative photographs of cells stained with phalloidin (red) and DAPI (blue) are shown. Scale bar, 10 μm. n = 4.

(F) Adhesion of neutrophils to iC3b under shear flow (0.38 dynes/cm^2) at the indicated time points. Results are presented as percent of adherent neutrophils relative to the non-risk donor at 10 min. n = 7–8 per genotype.

(G) Crawling velocity of neutrophils over a plasma-coated surface. n = 4 per genotype.

(H–J) Neutrophils from healthy volunteers were treated with CBRN1/6, CBRN 3/4, or CBRM1/32 antibodies to block specific β-propeller regions; CBRM1/29 to block the αI-domain; or CBR LFA1/7, a non-blocking antibody binding control. Cell adhesion under static (H) and shear flow (I) conditions, and crawling velocity (J) were evaluated. n = 4–6.

Data are mean ± SEM. See also Figure S1 and Table S1.

n.s., no statistical significance; *p < 0.05, **p < 0.01, ***p < 0.001 between neutrophils from non- and risk variants, and neutrophils with non-blocking versus blocking antibodies.

2013). We tested K562 cells expressing α_M^{WT} or α_M^{R77H} coupled to the β_2 subunit with or without the activating mutations V124A (Figure S3A) or L132A (data not shown) in adhesion assays to determine their ability to restore R77H binding defects. Both $\alpha_M^{WT}\beta_2^{V124A}$ and $\alpha_M^{R77H}\beta_2^{V124A}$ adopted an extended-open conformation in the absence of activating cations (Figure S3B), as predicted (Sen et al., 2013). However, α_M^{R77H} with β_2^{V124A} (Figure 2E) or β_2^{L132A} (data not shown) remained impaired in ligand binding under flow. The small molecule Leukadherin-1 (LA-1) binds and activates the αI domain without inducing global conformational changes (Faridi et al., 2013). Although LA-1 pre-treatment enhanced adhesion of α_M^{WT}-expressing cells (data not shown) as previously described (Faridi et al., 2013), it did not rescue the ability of α_M^{R77H} to bind iC3b under flow

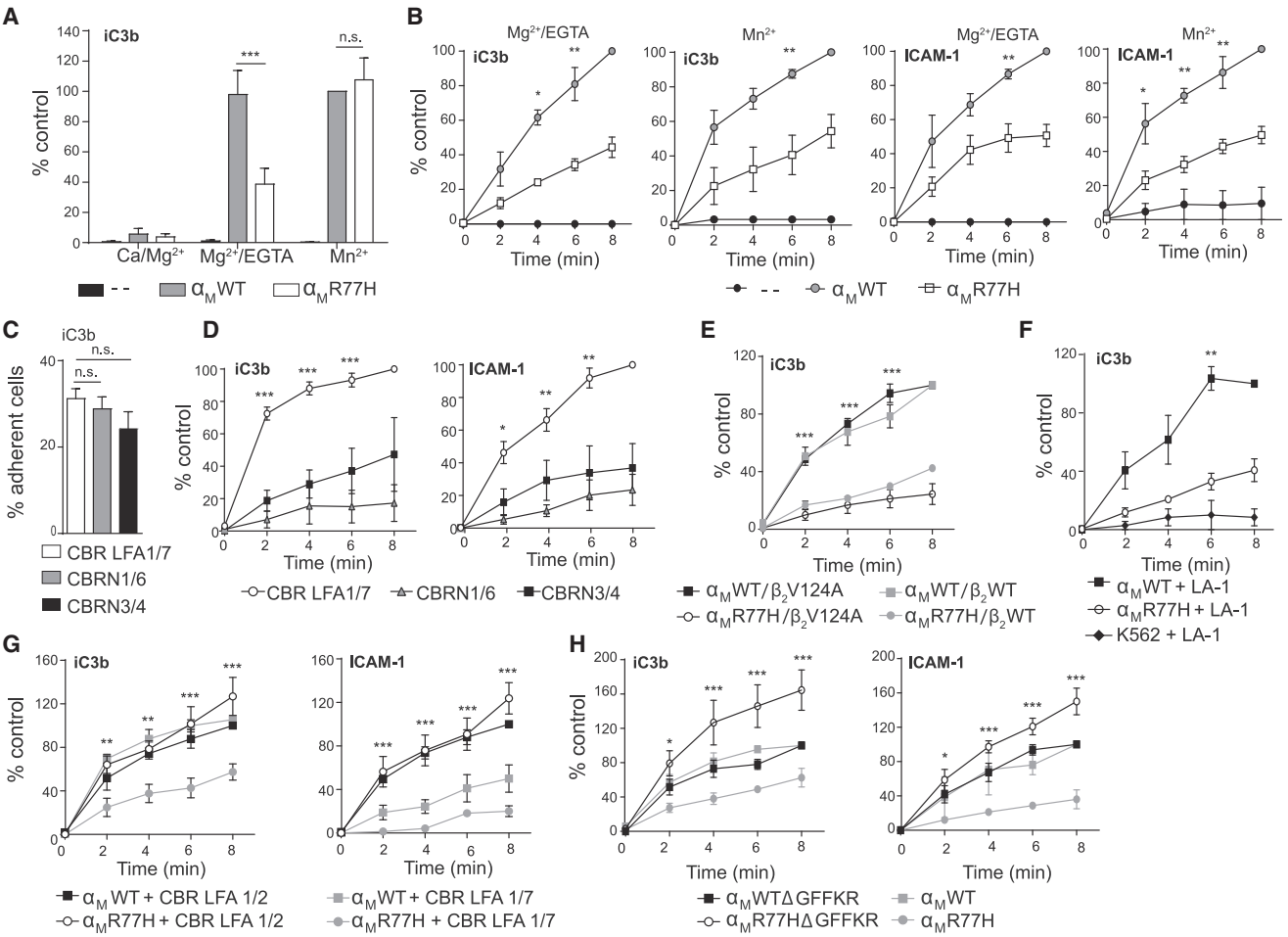

Figure 2. Functional Effects of Mac-1 R77H in K562 Cells

K562 cells lacking β_2 integrins (–) or stably expressing α_M^{WT} or α_M^{R77H} with β_2 were evaluated under static or flow conditions for adhesion to iC3b or ICAM-1 following activation with Mn^{2+} or Mg^{2+}/EGTA, respectively, unless otherwise indicated.

(A) Adhesion of α_M^{WT} or α_M^{R77H} cells to iC3b-coated surfaces under static conditions. Results are presented as percent of adherent cells relative to cells expressing α_M^{WT} plus Mn^{2+}. n = 6 experiments.

(B) Adhesion of α_M^{WT} or α_M^{R77H} cells to iC3b and ICAM-1 under shear flow (0.38 dynes/cm^2) evaluated at the indicated time points. Results are presented as percent of adherent cells relative to cells expressing α_M^{WT} at 8 min. n = 3–4 independent experiments.

(C and D) Binding of α_M^{WT} cells to ligand-coated surfaces following treatment with the indicated β-propeller antibodies (as in Figure 1) under static (C) or shear flow (D) conditions. n = 3–4.

(E) Cell adhesion under shear flow in cells expressing α_M^{WT} or α_M^{R77H} with β_2^{WT} or β_2^{V124A}.

(F and G) Adhesion of α_M^{WT} or α_M^{R77H} cells pretreated with leukoadherin-1 (LA-1) or vehicle control (F) or CBR LFA1/2 or the control antibody, CBR LFA1/7 (G).

(H) Adhesion of cells expressing α_M^{WT} or α_M^{R77H} with or without a GFFKR deletion (Δ). n = 3 for (E)–(H).

n.s., no statistical significance; *p < 0.05, **p < 0.01, ***p < 0.001 between αMWT and αMR77H (A–B), CBR LFA1/7 and other antibodies (D), αMWT/β2V124A and αMR77H/β2V124A (E), αMWT and αMR77H with LA-1 (F), αMR77H plus CBR LFA 1/2 versus 1/7 (G), and αMR77H and αMR77HΔGFFKR (H). Data are mean ± SEM. See also Figures S2 and S3 and Table S1.

(Figure 2F). Thus, neither an open, permissive βI domain nor direct activation of the αI domain rescues R77H.

Mn^{2+} and chemokine treatments favor integrin extension, but do not result in cytoplasmic tail separation (Kim et al., 2003; O'Brien et al., 2012). We exploited the CBR LFA1/2 antibody, which binds to the membrane proximal I-EGF-3 of the β_2 subunit (Lu et al., 2001) (see Figure 1A) and induces integrin extension (Petruzzelli et al., 1995) and cytoplasmic tail separation in both $\alpha_M\beta_2$ (Lefort et al., 2009) and $\alpha_L\beta_2$ (Kim et al., 2003). CBR LFA1/2 rescued the binding defect of α_M^{R77H} cells (Figure 2G).

To validate this conclusion, we deleted the α_M cytoplasmic tail and thus the GFFKR (ΔGFFKR) sequence, the mutation of which has been shown to result in tail separation and a fully extended, active integrin in the absence of activating cations (Kanse et al., 2004; Kim et al., 2003; Lu and Springer, 1997). Cells expressing $\alpha_M^{R77H\Delta GFFKR}$ resumed the ability to bind ligand under shear flow (Figure 2H). Unlike $\alpha_L\beta_2$ (Lu and Springer, 1997), ΔGFFKR in $\alpha_M\beta_2$ did not lead to constitutive extension and headpiece opening, but Mg^{2+}/EGTA or Mn^{2+} induced similar conformational changes in $\alpha_M^{R77H\Delta GFFKR}$ and $\alpha_M^{WT\Delta GFFKR}$ (Figures S3C and S3D). Thus,

forcing the tail and lower-leg separation of the α and β subunits, using both antibody and genetic approaches, restored adhesion in R77H cells.

R77H Reduces the Binding Affinity of Mac-1 at Zero Force by Decreasing Its On-Rate

To understand the effects of R77H on Mac-1's ligand-binding kinetics, we used a biomembrane force probe (BFP) (Figure 3A) to measure single-bond interactions between Mac-1-expressing cells and ICAM-1-bearing beads in the presence of Mg^{2+}/EGTA (Figure 3B). We analyzed the absence (Figure 3C, cyan) or presence (Figure 3C, magenta) of binding after a contact of given duration to obtain the adhesion frequency, and, when binding occurred, the lifetime of (most likely) a single bond under a desired force (Figure 3C). The adhesion frequencies of α_M^{WT} cells (Figure 3D, magenta circle) with ICAM-1 were higher than those of α_M^{R77H} (Figure 3D, cyan square) over a range of contact times, even though the α_M^{WT} cells had lower Mac-1 surface expression. An anti-αI-domain blocking antibody, CBRM1/29, abrogated adhesion, and streptavidin-coated beads blocked with bovine serum albumin (BSA) also showed rare adhesion events, confirming Mac-1 and ICAM-1 specificity (Figure 3D). The adhesion frequency versus contact time data were fit to Equation 1 in Supplemental Experimental Procedures along with the site densities m_r and m_l to evaluate the effective 2D affinities (Figure 3E) and stress-free off-rates (Figure 3F). R77H significantly reduced Mac-1 binding affinity, but not the off-rate (Figures 3E and 3F). Since affinity is the ratio of on-rate to off-rate, this indicates that R77H reduced the binding affinity of Mac-1 for ICAM-1 by reducing its on-rate. The lower affinity and on-rate of α_M^{R77H} versus α_M^{WT} at zero force provides a plausible explanation for the defect in static adhesion of α_M^{R77H} cells in the presence of Mg^{2+}/EGTA (Figure 2A).

Mac-1 R77H Suppresses Allosteric Catch Bonds

The mechanical regulation of Mac-1/ICAM-1 dissociation was quantified by the BFP. Zero-force bond lifetimes measured by thermal fluctuation were short and distributed as straight lines in semi-log survival frequency versus bond lifetime plots for both α_M^{WT} (Figure 3G) and α_M^{R77H} (Figure 3I). Their calculated off-rates were not significantly different (Figures 3G and 3I) and were comparable to the values obtained in the adhesion frequency assay (Figure 3F).

In contrast, the lifetimes of $\alpha_M\beta_2$/ICAM-1 bonds at low forces were distributed as two line segments in these semi-log plots, revealing two subpopulations of bonds (Figure 3G). The first subpopulation had fast dissociating rates, with off-rates comparable to the bonds at zero force. The second subpopulation had much slower dissociating rates, which equaled the negative slopes of the second line segments (Figure 3G). The slopes of the second line segments were much steeper (i.e., higher off-rates) for α_M^{R77H} (Figures 3I and 3J) than for α_M^{WT} (Figures 3G and 3H) at matched forces ($\geq$5 pN). Similar force induction of the slow-dissociating subpopulation of bonds has been observed for $\alpha_L\beta_2$/ICAM-1, which results in catch bonds (Chen et al., 2010; Xiang et al., 2011).

To examine whether Mac-1 forms catch bonds with ICAM-1, we plotted the bond lifetimes against force. For α_M^{WT}, as force increased, the lifetime first increased, reached the maximum at 12 pN, and then decreased, exhibiting a biphasic transition from catch to slip (Figure 3K). In comparison, the catch-slip trend of α_M^{R77H} was suppressed: the sharp summit in α_M^{WT} transformed into a relatively flat plateau with a 1-fold drop in amplitude, a leftward shift, and a marked shrinking of the catch regime to $\leq$5 pN, and a downward shift at the higher forces slip regime (Figure 3K). At ~12 pN, where α_M^{WT} reached the highest lifetime of 4 s, the α_M^{R77H} bond with ICAM-1 was 3-fold shorter-lived (~1 s). Catch bonds were attributed to $\alpha_M\beta_2$/ICAM-1 interactions because the rare adhesions of streptavidin-coated beads to α_M^{WT} cells in the presence of BSA alone showed negligible lifetimes under all forces (Figure S4A). Since under some conditions BSA can bind Mac-1 (Yalamanchili et al., 2000), polyvinylpyrrolidone (PVP) was used alternatively to block nonspecific binding, which yielded results similar to those obtained with BSA (Figure S4A), again suggesting that the short-lived bonds (Figures 3G–3J) do not stem from potential Mac-1/BSA interactions.

Therefore, R77H suppresses catch bonds, thus impairing the ability of cells to sustain their association with ICAM-1 under forces, but does not impact bond stability under force-free conditions. This is concordant with the adhesion assays, which show that R77H primarily impairs ligand binding under flow.

Rescue of Catch Bonds in Mac-1 R77H by the Activating Antibody CBR LFA1/2

CBR LFA1/2 treatment resulted in indistinguishable adhesion frequency versus contact time curves for α_M^{WT} and α_M^{R77H} (Figure S4B), with increased 2D affinities and reduced zero-force off-rates (Figures 3E and 3F) for both forms of Mac-1. Significantly, this antibody induced sizable subpopulations of slow-dissociating bonds with very long lifetimes over a wide range of forces for both α_M^{WT} (Figures S4E and S4F) and α_M^{R77H} (Figures S4G and S4H). This rendered an enhanced catch bond for α_M^{WT} with longer lifetimes under all forces than was obtained without the antibody (Figure 3L). The CBR LFA1/2 also increased the α_M^{R77H} bond lifetime and rescued the sharp catch-slip biphasic trend (Figure 3L). Notably, the two lifetime curves of α_M^{WT} and α_M^{R77H} overlapped under all forces, indicating that the impairment of the mutation on off-rate was completely overcome by CBR LFA1/2. The control antibody, CBR LFA1/7, confirmed the specificity of the activating effect of CBR LFA1/2 (Figure 3L).

Cytoplasmic Tail Separation Rescues the Catch Bond in R77H, whereas Activation of the βI Domain Has Only a Partial Effect

GFFKR deletion increased the 2D affinity and reduced the zero-force off-rate for α_M^{WT}, but not α_M^{R77H} (Figures 3E, 3F, and S4C). Nonetheless, $\alpha_M^{R77H\Delta GFFKR}$ rescued its impaired catch-slip trend (Figures 3M and S4I–S4L). The resulting lifetime curve overlapped well with those of CBR LFA1/2-activated cells (Figure 3L). This suggests a central role for cytoplasmic tail separation in transmitting allosteric signals within the α subunit for catch-bond formation.

Another mutation, β_2^{V124A}, which stabilizes the βI domain in an active state that is more permissive for internal ligand binding

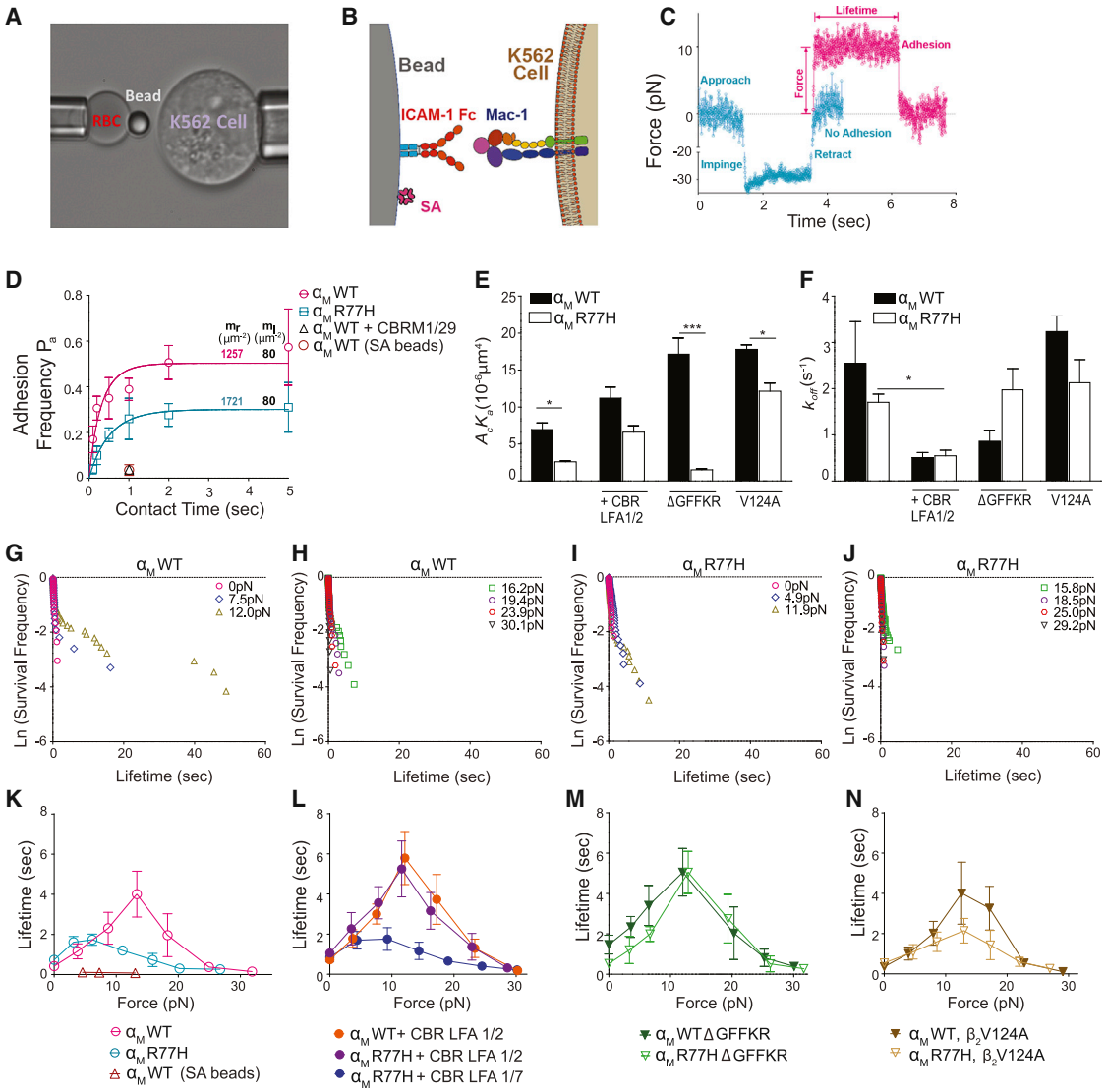

Figure 3. Characterization of Mac-1/ICAM-1 Binding Kinetics and Catch-Bond Formation by a BFP

(A) A micrograph of a BFP experiment is shown. A micropipette-aspirated RBC with an ICAM-1-coated probe bead attached to the apex (left) via biotin-streptavidin interaction was aligned against a target Mac-1-expressing K562 cell held by an opposing micropipette (right).

(B) A sketch of the probe bead double covalently coated with recombinant ICAM-1 and streptavidin, and the K562 cell expressing Mac-1.

(C) Superposition of force traces of two BFP contact cycles without (cyan) and with (magenta) an adhesion event. Without binding, the retraction curve returns to zero force upon target cell retraction. A contact cycle with adhesion, held at 10 pN, renders a lifetime until dissociation.

(D) Adhesion frequency-versus-contact time plot of the indicated cell lines. The site densities of Mac-1 (m_r) and ICAM-1 (m_l, 80 μm^{-2}) are marked along each curve. The binding frequencies of α_M^{WT}/ICAM-1 with either CBRM1/29 antibody (open black triangle) or streptavidin-coated beads (SA, open brown circle) at 1 s contact are shown.

(E and F) Effective 2D affinity (A_cK_a, E) and off-rate (k_{off}, F) of each Mac-1/ICAM-1 pair, calculated from fitting Equation 1 in Supplemental Experimental Procedures to the adhesion frequency data.

(G–J) Semi-log survival frequency versus bond lifetime plots of α_M^{WT} (G and H) and α_M^{R77H} (I and J) cells dissociating from the ICAM-1 bead under 0–12 pN (G and I) or >12 pN (H and J) forces. Survival frequency is calculated as the fraction of the binding events with a lifetime longer than a certain value t (sec).

(K–N) Plots of mean ± SEM bond lifetime versus force of α_M^{WT} and α_M^{R77H} cells dissociating from ICAM-1 beads in the absence (K) or presence (L) of CBR LFA1/2 or CBR LFA1/7 control antibody, or with a GFFKR deletion (M) or a β_2^{V124} mutation (N).

Data are mean ± SEM. See also Figure S4.

(Sen et al., 2013), resulted in a higher effective 2D affinity in cells expressing α_M^{WT} (Figures 3E and S4D). β_2^{V124A} expression with α_M^{R77H} not only rescued the deficiency of α_M^{R77H} in the 2D affinity but also increased it to a level higher than $\alpha_M^{WT}\beta_2^{WT}$ (Figure 3E). The β_2^{V124A} had minor effects on the off-rate of α_M^{R77H} and α_M^{WT} (Figures 3F and S4D), indicating that the affinity

increase resulted solely from the change in on-rate. Under force, V124A did not increase the peak lifetime of α_M^{R77H} (Figures 3N and S4M–S4P). However, the force regime of the ''catch'' phase was broadened to be similar to α_M^{WT}, indicating a partial rescue of the catch bond (Figure 3N). This partial rescue was not detected in the shear flow assay (Figure 2E), likely because off-rates and ligand densities also contribute to ligand-integrin interaction in this assay.

DISCUSSION

We demonstrate that the SLE-associated variant R77H in the Mac-1 α_M subunit (*ITGAM*) alters Mac-1's 2D affinity and its ability to form catch bonds, a counterintuitive strengthening of receptor-ligand bonds under mechanical forces. The latter provides a compelling explanation for the marked defect in this variant's ability to bind ligand, primarily under flow conditions. Thus, R77H does not lead to an overall reduction in Mac-1 ligand binding. Rather, R77 plays a regulatory role, which is consistent with the fact that it is outside the ligand-binding αI domain. The rescue of the R77H bond lifetime under force with activating antibodies or mutations that have been documented to induce allostery identifies a specific role for R77 in force-induced Mac-1 bond stability, a finding that adds another level of complexity to the regulation of integrin function. Moreover, the phenocopy of R77H with β-propeller antibodies indicates new roles for R77 and the domain in which it resides in integrin allostery transmission, which is of interest because the β subunit has primarily been reported to transmit the conformational changes associated with ligand binding (Schürpf and Springer, 2011).

To explain the allosteric modulation of catch bonds by R77H, we propose a model based on the force balance within the integrin and the interplay of two catch bonds (Figure 4). The force balance is between the total force, F, applied to the αI domain by ICAM-1, and two component forces, F_α and F_β, supported by the integrin α and β subunits, respectively (Figures 4C–4H). F_α transmits through the αI domain N terminus into the β-propeller domain near the lesion at R77, whereas F_β transmits through the αI domain α7 helix into the βI domain via the internal ligand (e.g., Figure 4C). The two catch bonds are (1) the external catch bond between the αI domain and ligand elicited by the total F, and (2) the internal catch bond between the αI and βI domains via the internal ligand elicited by component force F_β. These two catch bonds are coupled, as the external catch bond requires pulling of the αI domain α7 helix by the internal catch bond (Chen et al., 2010). The R77H mutation tilts the balance between the total force and the two component forces, resulting in a decrease in F_α and an increase in F_β (Figures 4C and 4D). This speeds up the increase of F_β with increasing F and results in an accelerated pulling of the αI domain α7 helix by F_β at still small F. This manifests as an early rise of the Mac-1/ligand catch bond with a longer lifetime for R77H than for the wild-type (WT) at 5 pN. A further increase in F ($F > 7$ pN) transitions the αI-βI interdomain interaction to a slip bond that is less able to pull on the αI domain α7 helix to elicit the external catch bond with ligand, thus resulting in an earlier transition from the catch- to slip-bond regime for R77H compared with WT (Figures 4C and 4D). This explains the compression of the force range F of the Mac-1/ligand catch bond from 0–12 pN for α_M^{WT} to 0–5 pN for α_M^{R77H} (Figure 3K).

CBR LFA1/2 maximally activates Mac-1 by inducing full integrin extension. Separation of the α and β tails occurs upon binding of this antibody or deletion of the α-subunit GFFKR sequence, both of which augmented the catch bond in α_M^{R77H} by force redistribution (Figures 4E and 4F). The Mac-1 αI domain exists in an equilibrium between closed/inactive and open/active states (Figures 4A–4C), transiently coupling the binding of the external ligand to the binding of its internal ligand to the βI domain. A catch bond with ligand requires F_β to pull on the α7 helix to activate the αI domain. We propose that cytoplasmic tail separation swings out the hybrid domain to activate the βI domain for binding of the internal ligand. The strengthened internal catch bond enables the allosteric relay between αI and βI domains, and supports a higher F_β to amplify (for WT) and rescue (for R77H) the Mac-1/ligand catch bond (Figures 4E and 4F).

The V124A mutation stabilizes the βI domain in an active state that is more permissive for internal ligand binding (Sen et al., 2013). Thus, the mechanism for the V124A mutation to broaden the force range of the αI-βI interdomain catch bond and to right-shift the lifetime-versus-force curve of the Mac-1/ligand catch bond may be qualitatively similar to but quantitatively less effective than that of the CBR LFA1/2 and ΔGFFKR for both α_M^{WT} and α_M^{R77H} (Figures 4G and 4H). The suppressed Mac-1/ligand catch bond in R77H resembles (albeit less dramatically) the altered lifetime-versus-force curve of $\alpha_L\beta_2$'s bond with ICAM-1 in the presence of XVA143 (Chen et al., 2010), a small-molecule antagonist that binds to the internal ligand-binding site on the βI domain and blocks the conformation signal relay between the αI and βI subunits (Shimaoka et al., 2003). How R77H may structurally affect the αI and βI interdomain communication required for catch bonds requires further study.

The *ITGAM*-R77H variant is a common allele in healthy populations (~10%). In non-autoimmune conditions, the influence of this variant may be minor due to the existence of many regulatory checkpoints. However, in SLE, where dysfunction of several aspects of the immune response occurs simultaneously, the R77H variant might impact disease. The possibility that the *ITGAM* variant R77H in linkage disequilibrium with a true causative mutation is responsible for the observed phenotypes is unlikely, as the defects observed in neutrophils expressing R77H, as well as other SNPs, were similar to those observed in a cell line with R77H alone. How would compromised Mac-1 2D affinity for ligand and catch-bond formation, as observed in the R77H variant, increase SLE susceptibility? In addition to its pro-inflammatory roles, Mac-1 has immunosuppressive functions and inhibits the signaling of immune cell receptors (Fagerholm et al., 2013) that have been implicated in SLE pathogenesis (Tsokos, 2011). The precise mechanisms through which Mac-1 exerts its downmodulatory effects remain to be determined; however, according to a concept currently being developed in other systems, monovalent and low avidity ligation of a receptor leads to inhibitory signaling, whereas multivalent ligation promotes activating signals (Blank et al., 2009; Ivashkiv, 2011). Thus, we propose that a reduction in Mac-1 2D ligand affinity in the absence of high-valency ligand may prevent Mac-1's inhibitory function. Furthermore, impaired stability of single receptor/ligand bonds

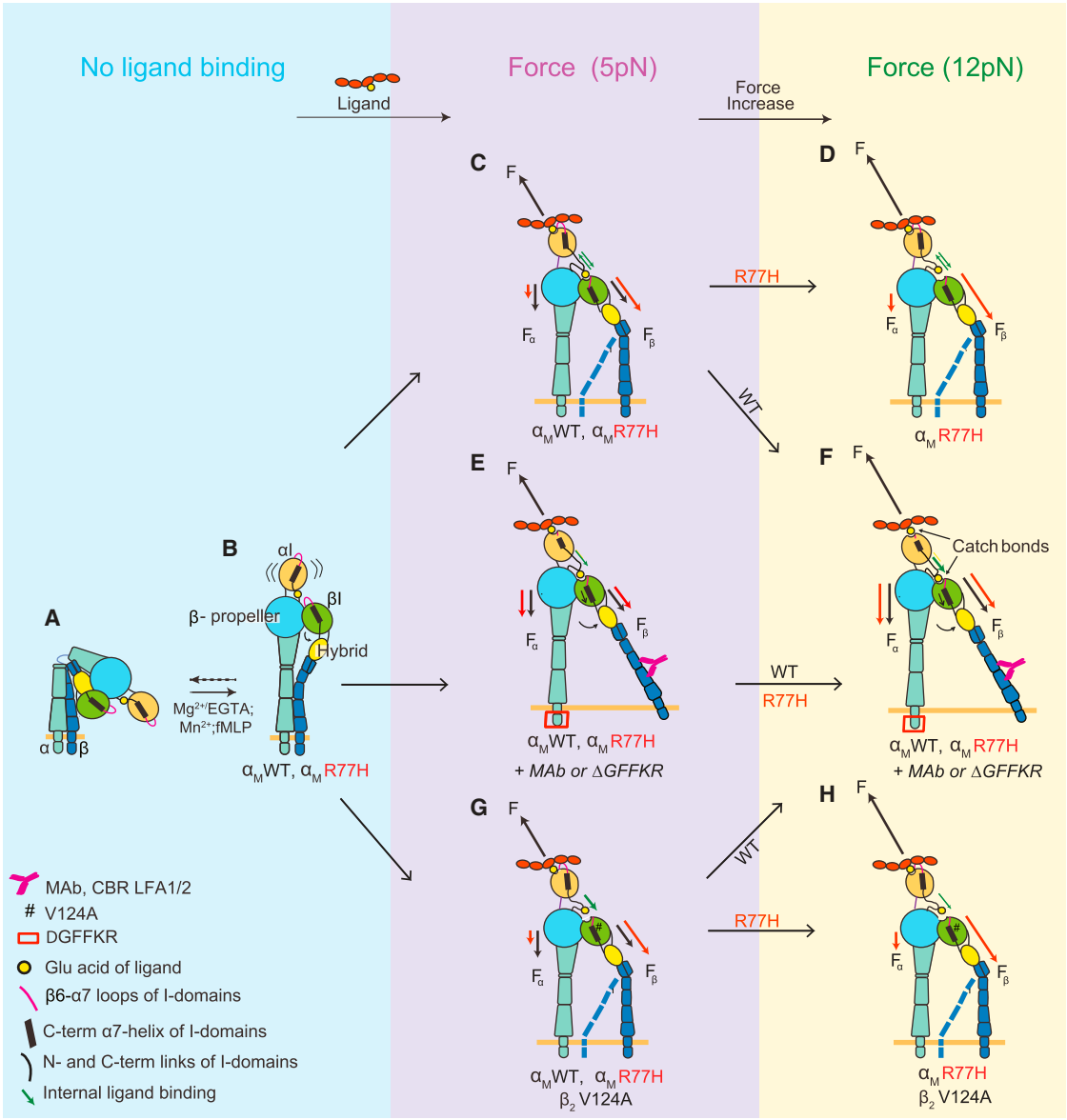

Figure 4. Model of How R77H Affects Ligand Binding and Catch-Bond Formation by Mac-1

(A) Inactive, bent Mac-1 with a closed headpiece. The αI domain is in the inactive conformation, with the α7 helix in the up position and the MIDAS in the closed conformation.

(B) Mac-1 extension induced by inside-out signaling (fMLP) or activating metal ions.

(C–H) Mac-1 under a lower (5 pN; C, E, and G) or higher (12 pN; D, F, and H) stretching force following ligand binding. The blue dotted line for CD18 in (C), (D), (G), and (H) depicts the cytoplasmic tail in a clasped (as in B) or unclasped position. Force (*F*) applied by the ligand and the component forces from the αI-domain MIDAS to the β-propeller (F_α) or the βI (F_β) domain are black for WT and red for R77H. R77H perturbs the force distribution so that more force is transmitted to the βI domain and induces a premature catch bond at lower force (C), while at the higher force F_β exceeds the optimal value for αI- and βI-domain interaction and results in a weaker binding capacity (D). Forced ectodomain extension and tail separation by CBR LFA1/2 antibody or deletion of the regulatory GFFKR of the α subunit restores the force redistribution in R77H and hence rescues R77H by swinging out the hybrid domain to activate the βI domain and strengthen the αI-βI interdomain catch bond to prolong the bond lifetime (E and F). The V124A mutation (#) moves the βI domain into a more activated state, resulting in more stable internal ligand binding (green arrow). This partially rescues the R77H catch-bond defect (H), but to a lesser extent, and hence does not fix the perturbed force distribution in R77H (G).

under mechanical force (catch bonds), in the absence of multivalent Mac-1 ligand engagement, may compromise inhibitory Mac-1 signaling. Mac-1 upregulation of FcγR functions is well known (Jones and Brown, 1996), but in models of lupus, an autoimmune disease characterized by high levels of immune complexes (Tsokos, 2011), Mac-1 deficiency leads to a significant increase in glomerular neutrophil accumulation and lupus nephritis (Kevil et al., 2004; Rosetti et al., 2012). The immunoglobulin G

(IgG)/immune complex receptor FcγRIIA mediates neutrophil adhesion to intravascular deposited soluble IgG-immune complexes (Tsuboi et al., 2008), which is enhanced by Mac-1 deficiency (Rosetti et al., 2012). During FcγRIIA-mediated neutrophil interactions with intravascular immune complexes, a defect in bond stability between Mac-1 R77H and ligand upon force exerted by blood flow could impact Mac-1's downregulatory function on FcγRIIA and thus augment neutrophil accumulation.

Allosteric catch bonds have been reported for several hematopoietic cell receptor/ligand pairs. Our data show that a Mac-1 variant that confers high risk for developing lupus alters the relay of allosteric signals required for catch bonds, suggesting that elimination of catch bonds may have pathological consequences.

EXPERIMENTAL PROCEDURES

Human Neutrophils, Lentiviral Constructs, and Generation of K562 Cell Lines

Genotyped human blood samples from *ITGAM* non-risk or risk variant (R77H)-carrying donors were provided by the Genotype and Phenotype Registry, a service of the Tissue Donation Program at The Feinstein Institute for Medical Research (Manhasset, NY). β-propeller antibodies were used on neutrophils from the blood of healthy volunteers under approved protocols (Brigham and Women's Hospital IRB). R77H and the GFFKR mutant (which was generated by including a stop codon before the GFFKR sequence) were generated in human α_M by PCR. β_2^{V124A} and β_2^{L132A} cDNA constructs were generated as previously described (Sen et al., 2013). All constructs were cloned into lentiviral plasmids (see Supplemental Experimental Procedures). K562 cells, which lack endogenous α_M and β_2, were transduced with lentiviruses and sorted for positive-expressing cells. Multiple clones expressing similar surface levels of Mac-1 were used in functional assays.

Static and Shear Flow Adhesion Assays

Integrin Activation

For Mg^{2+}/EGTA-induced activation, K652 cells were washed with Hank's balanced salt solution (HBSS) without Ca^{2+} and Mg^{2+} (Lonza) with 5 mM EDTA, washed again with HBSS, and resuspended in HBSS plus Mg^{2+}/EGTA (2 mM of each). For Mn^{2+}-induced activation, K562 cells were washed in HEPES plus 2 mM EGTA and 0.5 mM $MnCl_2$, and resuspended in HEPES/1 mM $MnCl_2$. Neutrophils were activated with 500 nM fMLP in PBS plus 2 mM Ca^{2+} and Mg^{2+}.

For details regarding ligand coating, see Supplemental Experimental Procedures.

Static Adhesion Assays

Cells were labeled with carboxyfluorescein succinimidyl ester (CFSE; Molecular Probes, Invitrogen) and placed on ligand-coated surfaces plus activating stimuli, and the percentage of adherent cells relative to α_M^{WT} cells treated with Mn^{2+} was calculated. For blocking experiments using the anti-β-propeller antibodies, the percent inhibition relative to CBR LFA1/7 control was calculated.

Shear Flow Adhesion Assay

Cells were perfused through a flow chamber at 1 dynes/cm^2 for a min. Shear flow was then decreased to 0.19–0.67 dynes/cm^2 and the number of cells that accumulated in four different fields after 2 min was calculated. Further details are provided in Supplemental Experimental Procedures.

Spreading and Crawling Assay

For details regarding the spreading and crawling assay, see Supplemental Experimental Procedures.

BFP

Details regarding the BFP have been previously described (Chen et al., 2008b). Details regarding RBC and bead preparation and BFP analysis are provided in Supplemental Experimental Procedures.

Adhesion Frequency Assay

An adhesion frequency assay reports the 2D binding kinetics between the receptor and ligand. For details, see Supplemental Experimental Procedures.

Thermal Fluctuation Assay

A thermal fluctuation assay was used for lifetime measurements under zero force (Chen et al., 2008a, 2010). The ICAM-1 coating densities of the beads were adjusted to achieve ≤20% adhesion frequency as required for single-bond adhesion events. Details are provided in Supplemental Experimental Procedures.

Force-Clamp Assay

A force-clamp assay was used to measure bond lifetimes under a constant force as previously described (Chen et al., 2010). Details are provided in Supplemental Experimental Procedures.

Lifetime Analysis

Lifetimes were categorized into bins of successive force ranges, each with a width of ~5 pN. The average lifetime in each force bin was collected to plot the lifetime curve as a function of the clamping force.

Statistical Analysis

All data are mean ± SEM. The statistical significance of the differences was determined by Student's t test. For group analysis, two-way ANOVA was used. If significant differences were shown, the data were subjected to Tukey's test for multiple comparisons, with $p < 0.05$ considered significant.

SUPPLEMENTAL INFORMATION

Supplemental Information includes Supplemental Experimental Procedures, four figures, and one table and can be found with this article online at http://dx.doi.org/10.1016/j.celrep.2015.02.037.

AUTHOR CONTRIBUTIONS

F.R., Y.C., E.T., V.A., and J.M.H. performed and analyzed experiments. F.R. generated the mutants and cell lines, and conducted experiments under static and flow conditions and the FACs analysis. Y.C. generated and analyzed the BFP data. M.S. constructed the Mac-1 structure. X.C. aided in generating mutants. F.W.L. gave advice regarding flow assays. F.R., Y.C., M.S., C.Z., and T.N.M. designed the study and wrote the manuscript.

ACKNOWLEDGMENTS

We thank Dr. T. Springer for providing β_2 antibodies. This work was supported by grants from the NIH (HL065095 to T.N.M., AI044902 to C.Z., and T32 HL007627 to F.R.), the Target Identification in Lupus Grant/Alliance for Lupus Research Foundation (to T.M.), the Consejo Nacional de Ciencia y Tecnologia and Fundación México en Harvard (to F.R.), and the German Research Foundation (HE-6810/1-1 to J.M.H.).

Received: July 25, 2014
Revised: October 26, 2014
Accepted: February 11, 2015
Published: March 12, 2015

REFERENCES

Abram, C.L., and Lowell, C.A. (2009). Leukocyte adhesion deficiency syndrome: a controversy solved. Immunol. Cell Biol. *87*, 440–442.

Blank, U., Launay, P., Benhamou, M., and Monteiro, R.C. (2009). Inhibitory ITAMs as novel regulators of immunity. Immunol. Rev. *232*, 59–71.

Carman, C.V., and Springer, T.A. (2003). Integrin avidity regulation: are changes in affinity and conformation underemphasized? Curr. Opin. Cell Biol. *15*, 547–556.

Chen, W., Evans, E.A., McEver, R.P., and Zhu, C. (2008a). Monitoring receptor-ligand interactions between surfaces by thermal fluctuations. Biophys. J. *94*, 694–701.

Chen, W., Zarnitsyna, V.I., Sarangapani, K.K., Huang, J., and Zhu, C. (2008b). Measuring receptor-ligand binding kinetics on cell surfaces: from adhesion frequency to thermal fluctuation methods. Cell. Mol. Bioeng. *1*, 276–288.

Chen, W., Lou, J., and Zhu, C. (2010). Forcing switch from short- to intermediate- and long-lived states of the alphaA domain generates LFA-1/ICAM-1 catch bonds. J. Biol. Chem. *285*, 35967–35978.

Choi, Y.I., Duke-Cohan, J.S., Chen, W., Liu, B., Rossy, J., Tabarin, T., Ju, L., Gui, J., Gaus, K., Zhu, C., and Reinherz, E.L. (2014). Dynamic control of β1 integrin adhesion by the plexinD1-sema3E axis. Proc. Natl. Acad. Sci. USA *111*, 379–384.

Fagerholm, S.C., MacPherson, M., James, M.J., Sevier-Guy, C., and Lau, C.S. (2013). The CD11b-integrin (ITGAM) and systemic lupus erythematosus. Lupus *22*, 657–663.

Faridi, M.H., Altintas, M.M., Gomez, C., Duque, J.C., Vazquez-Padron, R.I., and Gupta, V. (2013). Small molecule agonists of integrin CD11b/CD18 do not induce global conformational changes and are significantly better than activating antibodies in reducing vascular injury. Biochim. Biophys. Acta *1830*, 3696–3710.

Fiore, V.F., Ju, L., Chen, Y., Zhu, C., and Barker, T.H. (2014). Dynamic catch of a Thy-1-α5β1+syndecan-4 trimolecular complex. Nat. Commun. *5*, 4886.

Han, S., Kim-Howard, X., Deshmukh, H., Kamatani, Y., Viswanathan, P., Guthridge, J.M., Thomas, K., Kaufman, K.M., Ojwang, J., Rojas-Villarraga, A., et al. (2009). Evaluation of imputation-based association in and around the integrin-alpha-M (ITGAM) gene and replication of robust association between a non-synonymous functional variant within ITGAM and systemic lupus erythematosus (SLE). Hum. Mol. Genet. *18*, 1171–1180.

Hom, G., Graham, R.R., Modrek, B., Taylor, K.E., Ortmann, W., Garnier, S., Lee, A.T., Chung, S.A., Ferreira, R.C., Pant, P.V., et al. (2008). Association of systemic lupus erythematosus with C8orf13-BLK and ITGAM-ITGAX. N. Engl. J. Med. *358*, 900–909.

Ivashkiv, L.B. (2011). How ITAMs inhibit signaling. Sci. Signal. *4*, pe20.

Jones, S.L.B., and Brown, E.J. (1996). Functional cooperation between Fcg receptors and complement receptors in phagocytes. In Human IgG Fc Receptors, J.G.C. van de Winkel and P.J.A. Capel, eds. (R.G. Landes Co.), pp. 149–163.

Kanse, S.M., Matz, R.L., Preissner, K.T., and Peter, K. (2004). Promotion of leukocyte adhesion by a novel interaction between vitronectin and the beta2 integrin Mac-1 (alphaMbeta2, CD11b/CD18). Arterioscler. Thromb. Vasc. Biol. *24*, 2251–2256.

Kevil, C.G., Hicks, M.J., He, X., Zhang, J., Ballantyne, C.M., Raman, C., Schoeb, T.R., and Bullard, D.C. (2004). Loss of LFA-1, but not Mac-1, protects MRL/MpJ-Fas(lpr) mice from autoimmune disease. Am. J. Pathol. *165*, 609–616.

Kim, M., Carman, C.V., and Springer, T.A. (2003). Bidirectional transmembrane signaling by cytoplasmic domain separation in integrins. Science *301*, 1720–1725.

Kong, F., García, A.J., Mould, A.P., Humphries, M.J., and Zhu, C. (2009). Demonstration of catch bonds between an integrin and its ligand. J. Cell Biol. *185*, 1275–1284.

Lefort, C.T., Hyun, Y.M., Schultz, J.B., Law, F.Y., Waugh, R.E., Knauf, P.A., and Kim, M. (2009). Outside-in signal transmission by conformational changes in integrin Mac-1. J. Immunol. *183*, 6460–6468.

Liu, B., Chen, W., Evavold, B.D., and Zhu, C. (2014). Accumulation of dynamic catch bonds between TCR and agonist peptide-MHC triggers T cell signaling. Cell *157*, 357–368.

Lu, C.F., and Springer, T.A. (1997). The alpha subunit cytoplasmic domain regulates the assembly and adhesiveness of integrin lymphocyte function-associated antigen-1. J. Immunol. *159*, 268–278.

Lu, C., Ferzly, M., Takagi, J., and Springer, T.A. (2001). Epitope mapping of antibodies to the C-terminal region of the integrin beta 2 subunit reveals regions that become exposed upon receptor activation. J. Immunol. *166*, 5629–5637.

O'Brien, X.M., Heflin, K.E., Lavigne, L.M., Yu, K., Kim, M., Salomon, A.R., and Reichner, J.S. (2012). Lectin site ligation of CR3 induces conformational changes and signaling. J. Biol. Chem. *287*, 3337–3348.

Petruzzelli, L., Maduzia, L., and Springer, T.A. (1995). Activation of lymphocyte function-associated molecule-1 (CD11a/CD18) and Mac-1 (CD11b/CD18) mimicked by an antibody directed against CD18. J. Immunol. *155*, 854–866.

Phillipson, M., Heit, B., Colarusso, P., Liu, L., Ballantyne, C.M., and Kubes, P. (2006). Intraluminal crawling of neutrophils to emigration sites: a molecularly distinct process from adhesion in the recruitment cascade. J. Exp. Med. *203*, 2569–2575.

Rosetti, F., Tsuboi, N., Chen, K., Nishi, H., Ernandez, T., Sethi, S., Croce, K., Stavrakis, G., Alcocer-Varela, J., Gómez-Martin, D., et al. (2012). Human lupus serum induces neutrophil-mediated organ damage in mice that is enabled by Mac-1 deficiency. J. Immunol. *189*, 3714–3723.

Schürpf, T., and Springer, T.A. (2011). Regulation of integrin affinity on cell surfaces. EMBO J. *30*, 4712–4727.

Sen, M., Yuki, K., and Springer, T.A. (2013). An internal ligand-bound, metastable state of a leukocyte integrin, αXβ2. J. Cell Biol. *203*, 629–642.

Shimaoka, M., Salas, A., Yang, W., Weitz-Schmidt, G., and Springer, T.A. (2003). Small molecule integrin antagonists that bind to the beta2 subunit I-like domain and activate signals in one direction and block them in the other. Immunity *19*, 391–402.

Sokurenko, E.V., Vogel, V., and Thomas, W.E. (2008). Catch-bond mechanism of force-enhanced adhesion: counterintuitive, elusive, but … widespread? Cell Host Microbe *4*, 314–323.

Tsokos, G.C. (2011). Systemic lupus erythematosus. N. Engl. J. Med. *365*, 2110–2121.

Tsuboi, N., Asano, K., Lauterbach, M., and Mayadas, T.N. (2008). Human neutrophil Fcgamma receptors initiate and play specialized nonredundant roles in antibody-mediated inflammatory diseases. Immunity *28*, 833–846.

Xiang, X., Lee, C.Y., Li, T., Chen, W., Lou, J., and Zhu, C. (2011). Structural basis and kinetics of force-induced conformational changes of an αA domain-containing integrin. PLoS ONE *6*, e27946.

Xiao, T., Takagi, J., Coller, B.S., Wang, J.H., and Springer, T.A. (2004). Structural basis for allostery in integrins and binding to fibrinogen-mimetic therapeutics. Nature *432*, 59–67.

Xiong, J.P., Stehle, T., Goodman, S.L., and Arnaout, M.A. (2003). Integrins, cations and ligands: making the connection. J. Thromb. Haemost. *1*, 1642–1654.

Yalamanchili, P., Lu, C., Oxvig, C., and Springer, T.A. (2000). Folding and function of I domain-deleted Mac-1 and lymphocyte function-associated antigen-1. J. Biol. Chem. *275*, 21877–21882.

Yu, Y., Zhu, J., Mi, L.Z., Walz, T., Sun, H., Chen, J., and Springer, T.A. (2012). Structural specializations of α(4)β(7), an integrin that mediates rolling adhesion. J. Cell Biol. *196*, 131–146.

Zhou, Y., Wu, J., Kucik, D.F., White, N.B., Redden, D.T., Szalai, A.J., Bullard, D.C., and Edberg, J.C. (2013). Multiple lupus-associated ITGAM variants alter Mac-1 functions on neutrophils. Arthritis Rheum. *65*, 2907–2916.